Korean J. Chem. Eng., 34(2), 555-565 (2017)
DOI: 10.1007/s11814-016-0281-5

pISSN: 0256-1115
eISSN: 1975-7220

Successive growth and applications of polymeric particles with controllable size and shapes

Young-Sang Cho† and Cheol Hwan Shin

Department of Chemical Engineering and Biotechnology, Korea Polytechnic University, 237, Siheung-si, Gyeonggi-do 15073, Korea
(*Received 2 July 2016 • accepted 11 October 2016*)

Abstract−Nonspherical particles resembling sea pineapples were synthesized by successive growth technique during soapless emulsion polymerization for various applications. First, highly cross-linked seed particle dispersion was synthesized by emulsifier-free emulsion polymerization with acrylic acid as co-monomer for the formation of surface carboxylic groups. Then, a successive growth scheme was applied to the seeds by swelling the particles with monomer droplets, followed by polymerization. The sea pineapple-shaped particles could be produced by adjusting the amount of monomer during the swelling step of the third growth. As a demonstrative application, the seed or sea pineapple-shaped particles could be used as templates for the synthesis of porous inorganic particles by spray drying technique. The resulting porous particles could be adopted as photocatalyst for the decomposition of organic molecules such as methylene blue. As another application, the dye molecules could be adsorbed onto the second grown particles to produce dye-doped nanospheres. Finally, the sea pineapple-shaped particles could be self-organized into supra-aggregates using toluene emulsions as confining geometries. Collectively, successively grown particles were found to be efficient building blocks to prepare the unusually packed structures or functionalized into colored products.

Keywords: Nonspherical Particles, Monomer Swelling, Successive Growth, Emulsion Polymerization, Self-assembly

INTRODUCTION

After the replacement of natural rubber using polymer latex developed during World War II, emulsion polymerization schemes have been studied intensively for various applications, including traditional chemical industries such as adhesive products and novel material self-assembly such as colloidal photonic crystals [1-5]. Besides these applications, colloidal templating method has been developed using spherical polymeric particles with submicron size synthesized by emulsion polymerization [6-9]. Thus far, most of these applications have been studied using polymeric colloids with spherical morphologies, which could be achieved by conventional emulsion polymerization.

Usually, the morphology of the polymeric particles synthesized by emulsion polymerization is spherical since the interfacial tension between particles and surrounding medium can be minimized due to the spherical shape. However, it has been reported that the dumbbell and snowman-shaped particles as well as multi-pod shapes can be also fabricated by seeded emulsion polymerization, since phase separation of swollen monomer inside particles will generate anisotropic morphologies after subsequent polymerization at elevated temperature [10-13]. After the pioneering researches by El-Aasser and colleagues, anisotropic morphologies of polymeric colloids could be produced by seeded emulsion polymerization, and the Okubo research group has extended this approach to dispersion polymerization scheme [14].

Besides the synthesis of shape-anisotropic particles, the applications of such colloidal particles have been studied intensively in the field of condensed matter physics and colloid chemistry. Colloidal crystals with anisotropic particles as building blocks have been produced to obtain unusual photonic band gaps [15]. Despite these advances, the packing and organization of polymeric particles with anisotropic morphologies have not been studied profoundly using complex colloids with various morphologies.

Inspired by these previous researches, composite particles with protruding head composed of PMMA attached to PS body could be synthesized from commercial seed particles, and their self-organization has been studied by Surface Evolver simulation [16]. Recently, a more advanced synthesis technique was developed by adjusting the polymerization conditions, and various morphologies including ellipsoids or trimer shapes could be obtained by seeded emulsion polymerization [17-20]. These anisotropic particles could be applied as building blocks of colloidal self-organization and templating materials for the fabrication of porous materials by emulsion-assisted self-assembly. However, other nonspherical particles resembling sea pineapple or raspberry-shaped particles are rarely reported through the approaches of emulsion polymerization; the applications of such particles are still challenging in the field of particulate technology.

In the present study, we synthesized polymeric particles resembled sea pineapples by successive growth technique using batch-type emulsion polymerization reactor. The seed particles were swollen

†To whom correspondence should be addressed.
E-mail: yscho78@kpu.ac.kr, yscho78@gmail.com

with monomer droplets and polymerized at elevated temperature to synthesize the sea pineapple-shaped particles with anisotropic morphologies. As the application of grown particles, dye molecules were adsorbed onto the carboxylated polymeric nanospheres for potential uses in bio-sensing purposes. The seed particles could be also packed as colloidal crystal film with light reflecting properties. The particles could be adopted as templating materials for the fabrication of macroporous ceramic particles with high porosity for photocatalytic decomposition of water pollutants. Sea pineapple-shaped particles could be also self-organized into colloidal supra-aggregates using toluene emulsion droplets as confining geometries. The resultant porous particles and supraparticles were observed by electron microscope.

EXPERIMENTAL

1. Materials

De-ionized water (18.2 $M\Omega cm^{-1}$) was used as reaction medium for emulsion polymerization of cross-linked particles and generated by using distilled water system (direct Q-3 with pump, Millipore). For the synthesis of cross-linked polystyrene nanospheres, the monomer such as styrene (99%) was purchased from Daejung Chemicals. Divinylbenzene (80%) was used as cross-linker and purchased from Aldrich Chemicals. The initiator, potassium peroxosulfate (95%) was bought from Junsei Chemicals. Comonomer, such as acrylic acid, was bought from Samchun Chemicals. For the synthesis of dye-doped polystyrene nanospheres, rhodamine B was bought from Junsei Chemicals. During sol spray drying for the fabrication of porous silica or titania particles, silica and titania nanocolloid was purchased from Aldrich and Nanoamor, respectively. For the fabrication of supra-aggregates of sea pineapple-shaped particles, formamide (99.5%) was used as continuous phase and purchased from Samchun Chemicals. The emulsion stabilizer, Pluronic F127 was bought from Kanto Chemicals. For the dispersed phase, toluene (99.8%) was used and purchased from Sigma-Aldrich.

2. The Synthesis of Cross-linked Seed Particles by Emulsion Polymerization

Emulsion polymerization was performed to synthesize cross-linked polystyrene seed particles according to the compositions shown in Table 1. After styrene monomer and divinylbenzene cross-linker were added to 380-ml water contained in batch-type reactor, nitrogen was fed to the reactor under vigorous stirring at 300 rpm for the deaeration of the reaction medium. Comonomer such as acrylic acid was also fed to the reactor for the surface functionalization. Then, the initiator (potassium peroxosulfate, KPS) mixed with 13.75-ml water was added to the reaction at elevated temperature such as 90 °C. The reaction was performed for 20 hours and the final polymeric seed particles were filtered to remove agglomerated powder.

3. Successive Growth of the Cross-linked Seed Particles

The seed particle dispersion was added to the batch-type polymerization reactor containing 292-ml distilled water under stirring at 300 rpm. Then, additional monomer mixture composed of styrene and divinylbenzene was added to the reactor while nitrogen gas was fed to the reaction system at elevated temperature such as 70 °C. After deoxygenation for 1.5 hours, seeded growth was performed by the addition of initiator such as KPS for about 20 hours to synthesize grown particle dispersion. The detailed successive growth conditions are summarized in Table 2.

4. The Fabrication of Colloidal Crystal Film Using Polystyrene Nanospheres

The dispersion of cross-linked polystyrene latex spheres synthesized by the first growth polymerization was dried inside UV cell at 60 °C for the fabrication of colloidal crystal film. The drying process continued for one day and the light-reflecting properties of the resulting colloidal crystal film was analyzed using UV-visible

Table 1. The synthesis conditions of seed particles by emulsifier free emulsion polymerization

Sample	KPS	Water	Styrene	DVB	Acrylic acid	Size
Seed	0.196 g	393.75 ml	10.75 ml	2.15 ml	2.3625 g	160 nm

Table 2. The conditions of the seeded growth steps by emulsifier free emulsion polymerization

Sample	KPS	Water	Styrene (or MMA)	DVB	Seed particles	Comment	Particle shape	Particle size (nm)
#1	0.196 g	305.75 ml	10.75 ml (Styrene)	2.15 ml	88 ml (Seed)	1st growth	Sphere	250
#2	0.196 g	305.75 ml	10.75 ml (Styrene)	2.15 ml	88 ml (#1)	2nd growth	Sphere	416
#3-1	0.098 g	305.75 ml	5.375 ml (Styrene)	1.075 ml	88 ml (#2)	3rd growth	Potato-like	584
#3-2	0.196 g	305.75 ml	10.75 ml (Styrene)	2.15 ml	88 ml (#2)	3rd growth	Sea pineapple-like	745
#4	0.196 g	305.75 ml	10.75 ml (Styrene)	2.15 ml	88 ml (#1)	2nd growth	Raspberry-like	436.3

Table 3. The conditions of the seeded growth steps for spherical latex beads

Sample	KPS	Water	Styrene	DVB	Seed particles	Comment	Particle shape	Particle size (nm)
#1	0.16205 g	393.75 ml	21.6 ml	4.86 ml	88 ml (Seed)	Seed	Sphere	267.5 nm
#2	0.32375 g	305.75 ml	44 ml	0.5457 ml	88 ml (#1)	1st growth	Sphere	751.0 nm
#3	0.32375 g	305.75 ml	44 ml	0.5457 ml	88 ml (#2)	2nd growth	Sphere	1205 nm

spectrophotometer.

5. The Adsorption of Rhodamine B Dyes on the Surface of Polystyrene Nanospheres

Cross-linked polystyrene latex spheres synthesized by the second growth polymerization were mixed with the aqueous solution of the dye molecules by stirring for 30 minutes. The resulting mixture was centrifuged for the isolation of the dye-doped polystyrene nanospheres by physisorption. The washing procedure was repeated two times and the final sediments were redispersed in fresh water by sonication.

6. The Synthesis of Supra-aggregates of Nonspherical Particles

The nonspherical particles resembling sea pineapples were suspended in ethanol by centrifugation and redispersion. The dispersion medium was replaced with toluene by another centrifugation and redispersion step to prepare the toluene dispersion of the nonspherical particles. The resulting dispersion was emulsified into aqueous solution of Pluronic F127 by mechanical homogenizer (DAIHAN, HG-15A-SET-A), followed by evaporation by heating at 90 °C for the evaporation of the toluene droplets to prepare the supra-aggregates of the cross-linked particles. The sample was washed several times by sedimentation under gravitational force and redispersion in fresh water for the removal of adsorbed surfactant.

7. The Synthesis of Macroporous Inorganic Micro-particles by Self-assembly

Cross-linked polystyrene latex spheres or sea pineapple-shaped particles were mixed with silica nano-colloid (Ludox HS-40) or commercial titania nanoparticles (Nanoamor) for the preparation of the feed solution to spray drying apparatus. Then, spray drying process was performed at 200 °C for the formation of organic-inorganic hybrid micro-particles, followed by calcination for the removal of polymeric particles. The calcination was carried out at 500 °C for five hours, and the final porous particles were applied as photocatalysts.

8. The Removal of Organic Pollutants from Water by Photocatalytic Degradation

The porous titania particles fabricated by spray drying technique were dispersed in water by mild sonication for a few seconds, and mixed with the aqueous solution of methylene blue solution. UV light from four UV lamps was irradiated to the solution mixture composed of titania catalyst and dye molecules for the photocatalytic decomposition of the organic molecules. The concentration of the dye was monitored as a function of UV irradiation time using UV-visible spectrometer, and the rate constant was evaluated assuming the first order reaction kinetics. Detailed procedures can be found elsewhere [21].

9. Characterizations

The particle size and distribution of the latex dispersion were measured by particle size analyzer (ZETA PLUS, Malvern Instruments). The morphologies of the seed particles and further grown particles were observed using field emission scanning electron microscope (FE-SEM, Hitachi-S4700). The morphologies of the macroporous ceramic particles and supra-aggregates of nonspherical particles were also observed with the electron microscope. The visible light absorbance and transmittance were measured by using UV-visible spectrometer (OPTIZEN POP).

RESULTS AND DISCUSSION

Fig. 1 contains the schematic for the synthesis of nonspherical particles by successive growth of cross-linked seed particles. In this article, cross-linked polystyrene nanospheres were synthesized as seed particles with high cross-linking density by soapless emulsion polymerization. From this dispersion of the seed particles, successive polymerization was performed by the addition of monomer

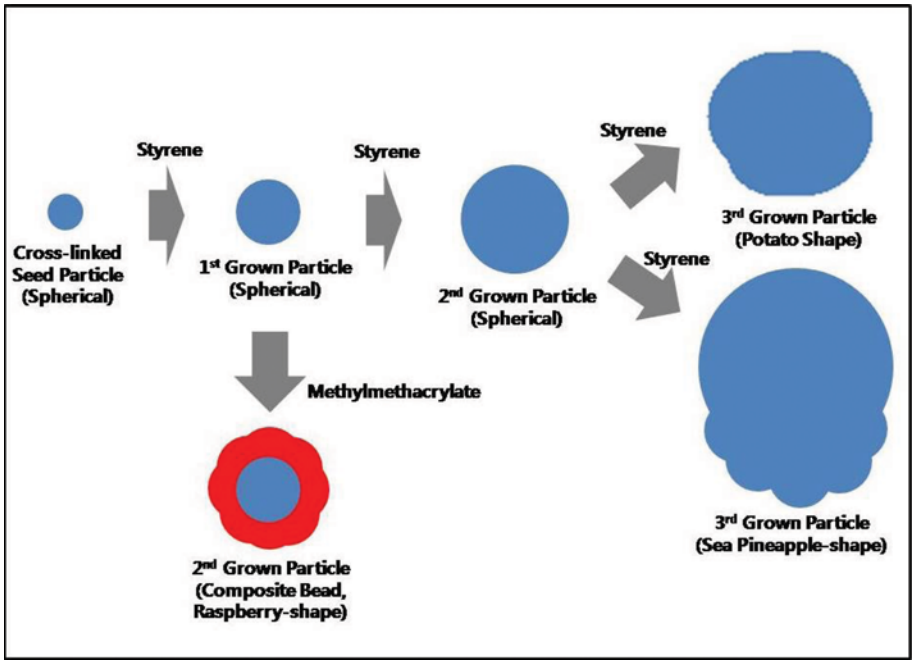

Fig. 1. Schematic for the successive growth of seed particles for nonspherical particles by seeded growth technique.

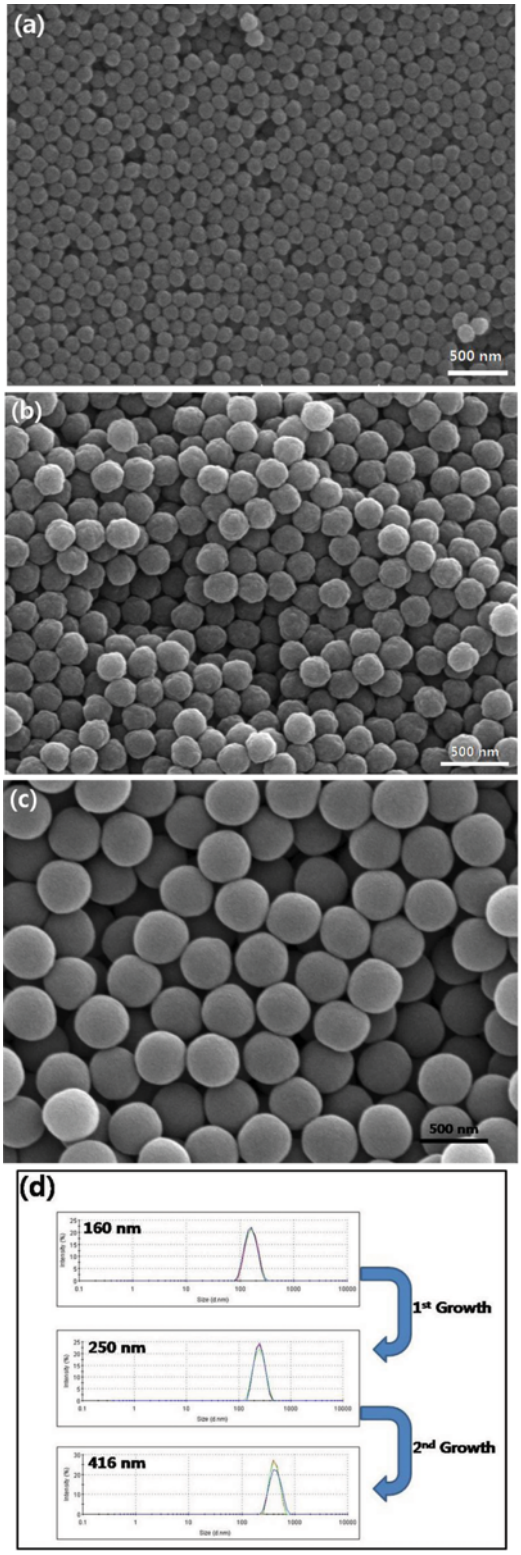

Fig. 2. Scanning electron microscope image of (a) seed particle dispersion synthesized using 16.7 vol% of DVB as cross-linker. The average particle size was measured as 160 nm. The scanning electron microscope image of (b) the grown particles using 12.9 ml of monomer by the first and (c) the second growth step. Scale bars indicate 500 nm. (d) The size distribution of seed particles, the first grown particles, and the second grown particles.

droplets followed by seeded emulsion polymerization to produce grown particles. The spherical morphology of the particles could be maintained until the second growth step, only causing the increase of the particle diameter. However, nonspherical sea pineapple-shaped particles could be produced from the third growth step, depending on the volume of monomer during swelling step, as depicted in Fig. 1. Composite particles could be also produced by the swelling of the 1st grown particles using methylmethacrylate monomer and successive polymerization at elevated temperature.

Fig. 2(a) contains the scanning electron microscope image of the cross-linked seed particles synthesized by acrylic acid as comonomer. 16.67 vol% of divinylbenzene was used as cross-linker during emulsifier-free emulsion polymerization, as summarized in the reaction conditions shown in Table 1. The seed particles are spherical with 160 nm in diameter. To control the size of the polystyrene nanospheres, successive polymerization was performed using the seed particles as starting materials by the addition of the monomer mixture of styrene and divinylbenzene, followed by the addition of initiator at elevated temperature such as 70 °C, as described in the conditions of Table 2. After the first growth step, the particles became larger with 250 nm in diameter, as displayed in the electron microscope image of Fig. 2(b), and the spherical morphologies were maintained for grown particles. A second growth was also performed to prepare larger particles by seeded growth technique, resulting in the bigger spherical particles shown in Fig. 2(c). As displayed in the particle size distribution graphs of Fig. 2(d), the diameter of the second grown particles increased from 250 to 416 nm, since the swelling of the particles by liquid monomers increased the size of the seed particles during the seeded growth step. There is clear coincidence between the particle size measured by light scattering technique and SEM observation, indicating that the dispersion of particles is quite stable without flocculants or aggregation.

Since acrylic acid was used as comonomer to synthesize the cross-linked polystyrene seed particles, it is evident that the surface of the particles might be covered with hydrophilic carboxyl groups derived from the comonomer. The surface functional groups can be confirmed using FT-IR spectrum of the seed particles from the characteristic peak at 1,704.9 cm^{-1} originating from the stretching vibration of the carbonyl groups, as shown in the solid line in the graph of Fig. 3(a). The strong peak at 1,600.8 cm^{-1} corresponds to the stretching vibration of benzene ring of polystyrene nanospheres. Thus, the seed particles can be used for the adsorption of biomolecules such as proteins, which are useful for the detection of various diseases [22].

For the first and second grown particles, the carboxylic groups could be detected as displayed in the spectrum of Fig. 3(a). However, the characteristic peak at 1,704.9 cm^{-1} might be attributed to the presence of the surface carboxylic groups on the seed particle surface, since FT-IR is bulk characterization method rather than surface analysis tool. To study the effect of the acrylic acid on the step growth, the first and second growth were conducted again by the same synthesis conditions described in Table 1, except the use of 2.3625 g of acrylic acid during emulsion polymerization. Thus, the final particle diameter was measured as 250 and 284.5 nm for the first and second grown particles, respectively. Especially for the

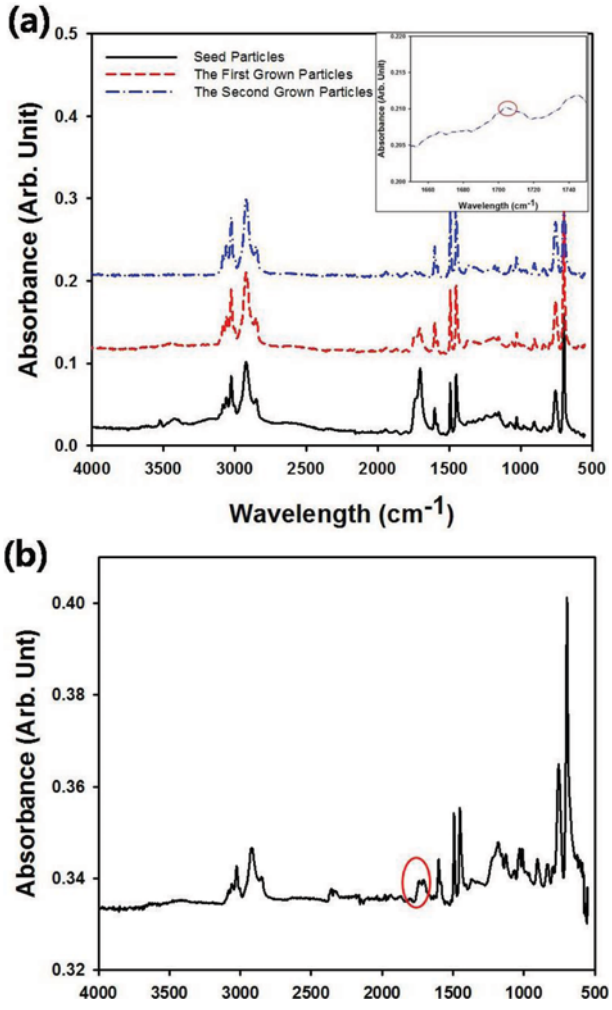

Fig. 3. (a) FT-IR spectrum of the seed, the first, and the second grown particles synthesized according to the conditions in Table 1. The inset figure is the magnified spectrum of the second grown particles near 1,704.9 cm^{-1}. (b) FT-IR spectrum of the second grown particles synthesized using acrylic acid as co-monomer.

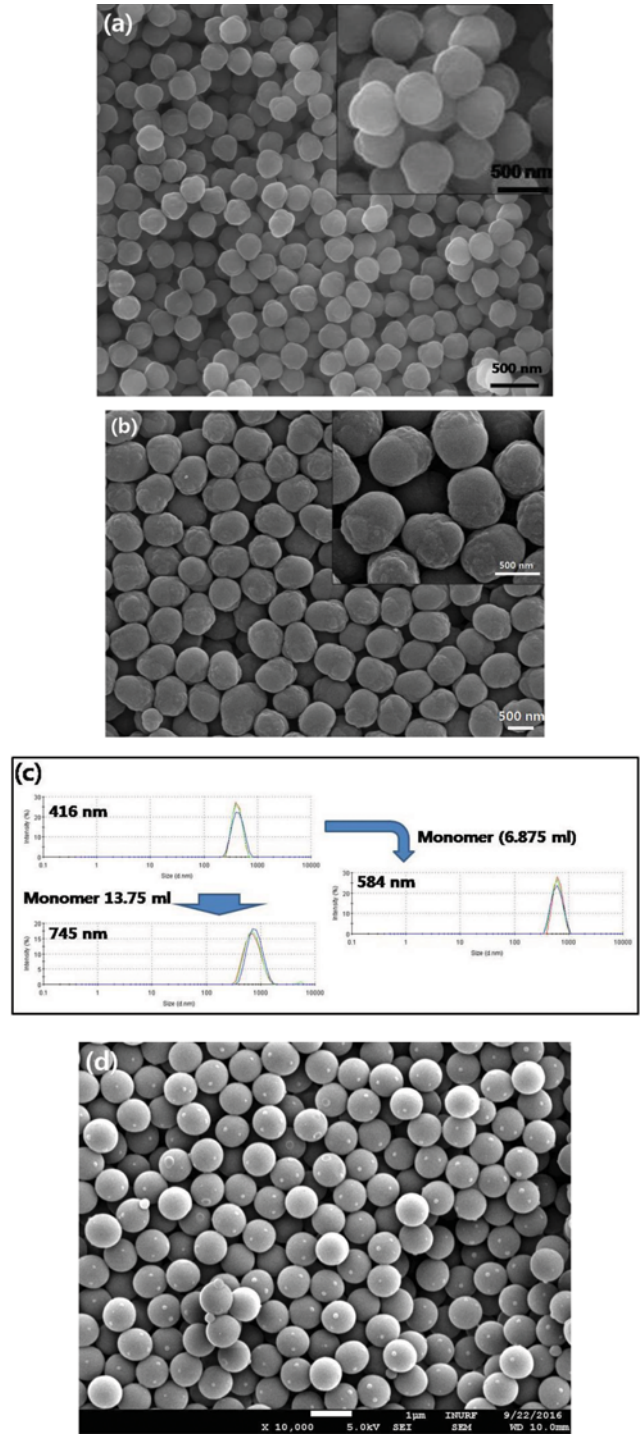

Fig. 4. Scanning electron microscope image of the third grown particles by the addition of (a) 6.45 and (b) 10.75 ml of monomer mixture. Scale bars indicate 500 nm. (c) The size distribution of the third grown particles shown in the SEM image of Fig. 4(a) and 4(b). (d) Scanning electron microscope image of the polystyrene microspheres (second grown particles) with spherical morphologies synthesized by the conditions shown in Table 2. Scale bar indicates 1 μm.

second grown particles, the particle diameter was reduced significantly compared to the size of the second grown particles synthesized without using comonomer such as acrylic acid due to the stabilizing effect of the comonomer. Thus, the surface carboxyl groups resulted in the decrease of the particle diameter during seeded emulsion polymerization. The FT-IR spectrum of the second grown particles fabricated using acrylic acid, is displayed in Fig. 3(b), indicating that the relative peak intensity around 1704.9 cm^{-1} was increased compared to the second grown particles synthesized without using the comonomer.

Besides the diameter of particles, the morphology of the polymeric particles was also controlled by successive polymerization of the second grown particles shown in Fig. 2(c). After the addition of monomer mixture, the particle shapes could be controlled as potato-like or sea pineapple-like morphologies, depending on the volume of monomer during swelling step. When a small amount of monomer mixture was added to the second grown particles, anisotropic particles could not be produced resulting in the irregular-shaped morphologies displayed in the scanning electron micro-

scope image of Fig. 4(a). However, highly anisotropic particles could be synthesized by increasing the amount of monomer during the seeded growth step, as shown in the electron microscope image of Fig. 4(b). The particle shapes became highly anisotropic due to the repelling of the excessive amount of monomer droplets from the cross-linked particles during swelling and subsequent polymerization step, since increased amount of monomer volume (sample #3-2) resulted in the formation of anisotropic particles, such as the morphologies of sea-pineapple. However, small amount of monomer volume caused isotropic particles (sample #3-1) although the shape was not perfectly spherical. It is evident that monomer-swollen particles were grown into highly anisotropic particles, since the monomer droplets suspended in solution separated from the seed particles may cause secondary particles with smaller diameter. In this study, the monomodal size of the particles and uniform particle morphology were observed after every growth step of the particles from particle size analysis and SEM observation, respectively. Thus, it can be concluded that the monomer swelling the seed particles resulted in the formation of the anisotropic particles.

Micron-sized polystyrene particles with spherical morphology could be also synthesized by step growth method. Table 2 summarizes the experimental conditions for the synthesis of the spherical polystyrene particles by seeded growth. During the step growth, the morphologies of the particles were maintained as spheres, and the SEM image of the second-grown particles are displayed in Fig. 4(d). It is thought that spherical particles could be obtained since the cross-linking density was low enough to induce the isotropic swelling of the monomer-swollen particles during the seeded growth step.

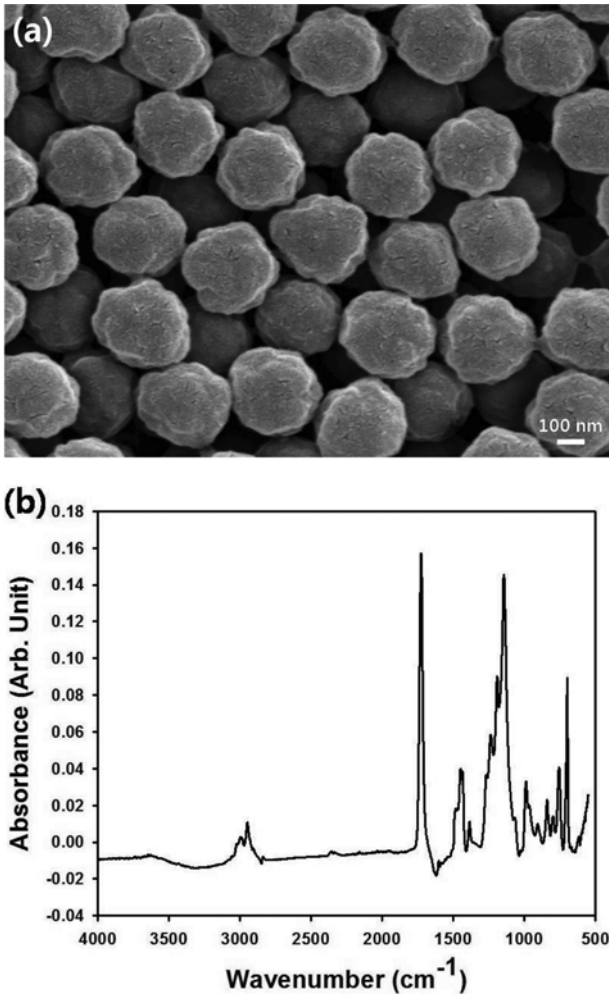

Fig. 5. (a) Scanning electron microscope image of PS-PMMA composite nanospheres. Scale bar indicates 100 nm. (b) FT-IR spectrum of PS-PMMA composite nanospheres.

Fig. 5(a) contains the scanning electron microscope image of PS-PMMA composite nanospheres. The dispersion of the first-grown polystyrene particles shown in Fig. 2(b) was used as seed particle suspension, and methylmethacrylate (MMA) was added for the swelling of the seeds. After swelling, subsequent polymerization at elevated temperature was performed to produce the PS-PMMA composite particles according to the conditions summarized as 'sample #5' in Table 2. The diameter of the polymeric beads was measured as 436.3 nm, which is comparable to the size of the second-grown polystyrene nanospheres displayed in Fig. 2(c). As displayed in Fig. 5(a), the morphologies of the composite particles are spheroids with multiple protrusions which resemble raspberry shapes. Since MMA monomer is not very compatible with polystyrene particles, some portion of monomer droplets are not fully contained in the cross-linked polystyrene beads, resulting in the formation of small protrusion on the surface of the PS-PMMA composite particles. Thus, surface roughness of the composite beads increased compared to the pure polystyrene nanospheres displayed in Fig. 2(c).

The formation of protrusion on the cross-linked particles can be considered using thermodynamic concept such as Gibbs energy. The chemical potential of the monomer droplets in the particles, $\Delta G_{m,P}$, can be explained as the summation of three contributions, including the monomer-particle mixing force (ΔG_m), the elastic retractile force of the cross-linked particle (ΔG_{el}), and the interfacial tension between the particle and reaction medium (ΔG_t), according to the following equation [23].

$$\Delta G_{m,P}=\Delta G_m+\Delta G_{el}+\Delta G_t \quad (1)$$

When $\Delta G_{m,P}$ is positive, protrusions will be formed from the seed particle surface during the seeded emulsion polymerization step. The contributions of ΔG_{el} and ΔG_t to $\Delta G_{m,P}$ are positive, whereas ΔG_m makes negative contribution for the formation of protrusions from the monomer-swollen particles. Since MMA monomer is not fully compatible with cross-linked polystyrene seed particles, ΔG_m will be increased, causing the formation of small protrusions from the particle surface after seeded emulsion polymerization.

Fig. 5(b) contains the FT-IR spectrum of PS-PMMA composite nanospheres displayed in Fig. 5(a). The characteristic peak of polymethylmethacrylate appeared at around 1,730 cm^{-1}, which is attributed to the carbonyl carbon of methylmethacrylate groups [24]. Other peak at around 1,200 cm^{-1} was observed due to C-O-C bonds of PMMA, indicating that PS-PMMA composite beads could be prepared from the seed particles of polystyrene nanospheres.

Fig. 6 contains the visible light spectrum of the colloidal crystal film fabricated using the first grown particles shown in Fig. 2(b). The absorbance and transmittance spectrums were measured, and

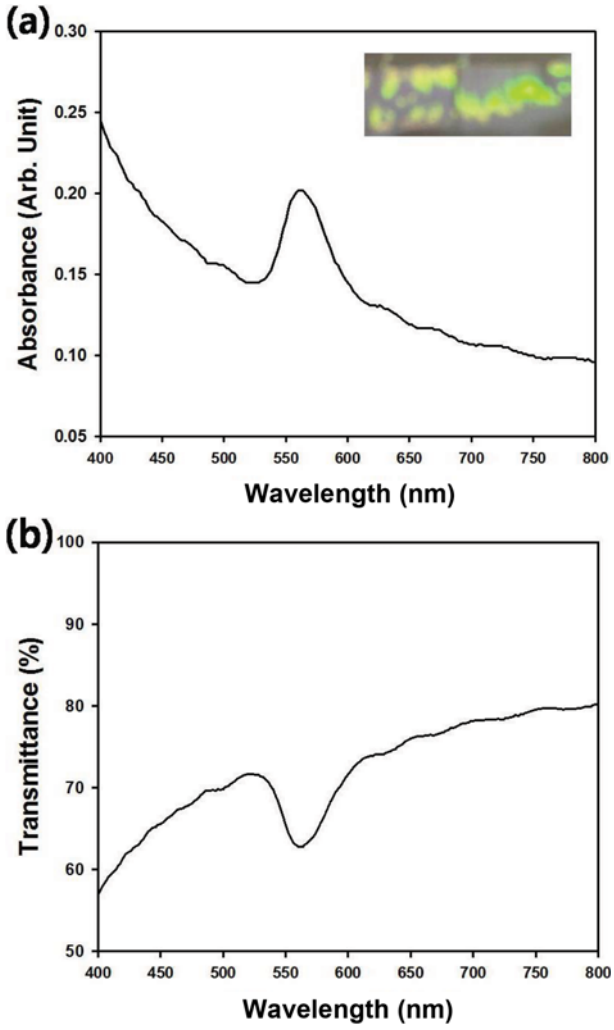

Fig. 6. (a) UV-visible absorbance and (b) transmittance spectrum of the second grown particles dried inside oven at 60 °C.

displayed in Fig. 6(a) and 6(b), respectively, indicating that the photonic band gap can be confirmed from the maximum or minimum peak position at around 565 nm. The peak position λ_{max} of spectrums can be theoretically predicted by the following Bragg diffraction equations:

$$\lambda_{max} = 2dn_{eff}\sqrt{1-\frac{\sin^2\theta}{n_{eff}^2}} \quad (2)$$

$$n_{eff}^2 = f_1 n_1^2 + f_2 n_2^2 \quad (3)$$

$$d = \sqrt{\frac{2}{3}}D \quad (4)$$

Here, n_1, n_2, and n_{eff} denote the refractive index of polystyrene, air, and the effective medium, respectively. The incident angle of light, θ, is 0° for normal incidence. In Eq. (2), f_1 and f_2 represent the packing fraction of polystyrene and air, respectively. The lattice spacing d can be predicted by using the particle diameter D from Eq. (3). For face-centered cubic lattice, the packing fraction of polystyrene nanospheres, f_1 is about 0.76 and f_2 should be 0.24. Thus, the particle size D can be predicted from the peak wavelength, λ_{max}=

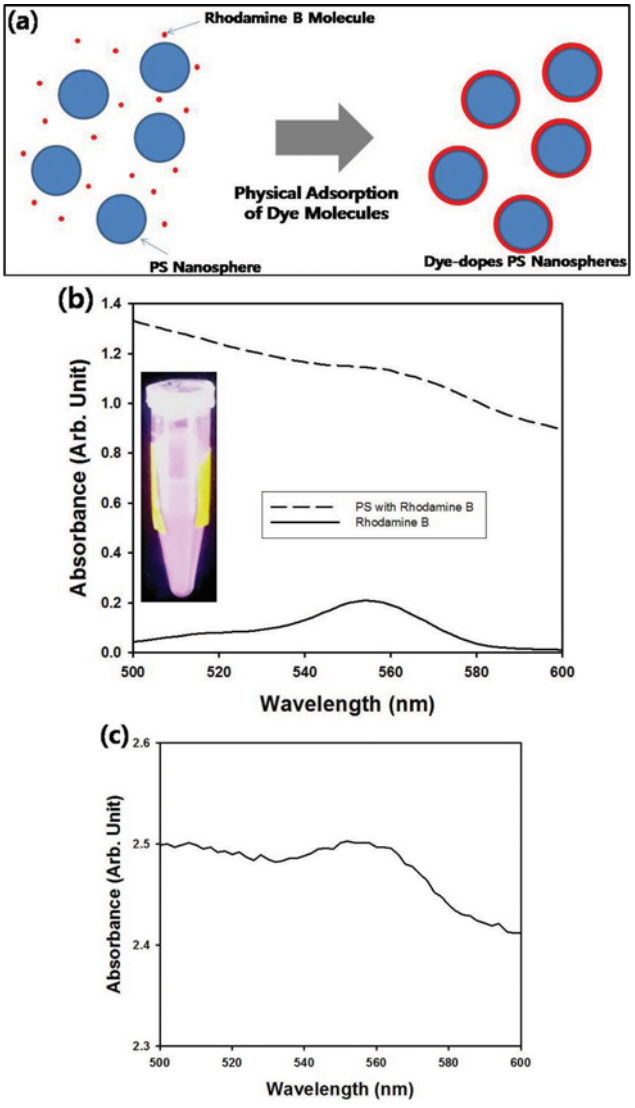

Fig. 7. (a) Schematic for the fabrication of dye-doped polymeric nanospheres by physical adsorption of Rhodamine B on the particle surface. (b) The UV-visible spectrum of the particle suspension (the second grown particles in Table 1). The inset photograph displays the polymeric dispersion of the dye-doped nanospheres. (c) The UV-visible spectrum of the dye-adsorbed particle suspension (the third grown particles).

565 nm, and the predicted value as 237 nm is close to the diameter measured from the SEM observation (250 nm). The ordered packing structure of polystyrene nanospheres, namely, colloidal crystal, could be fabricated by drying the colloidal dispersion of the monodisperse polystyrene nanospheres at 60 °C; the photograph of the sample is shown in the inset figure of Fig. 6(a). Green color can be observed from the colloidal crystal sample due to photonic band gap.

As an application of the polystyrene nanospheres displayed in Fig. 2(c), rhodamine B molecules were adsorbed on the particle surfaces, as depicted schematically in Fig. 7(a). For this purpose, the aqueous dispersions of the dye molecules and polystyrene nanospheres with 416 nm in diameter (the second grown particles in

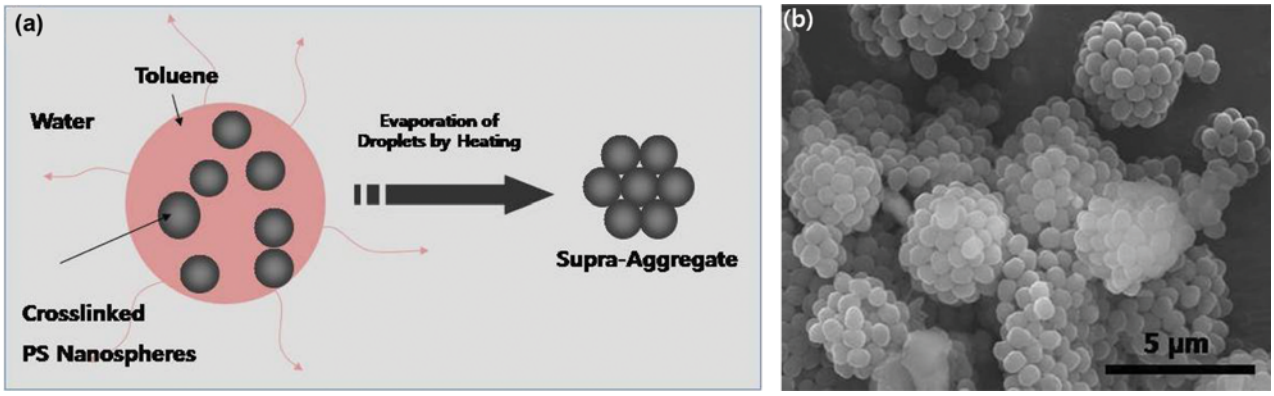

Fig. 8. (a) Schematic for the fabrication and (b) scanning electron microscope image of self-organized supra-particles of nonspherical polymeric particles shown in the SEM image of Fig. 4(b). Scale bar indicates 5 μm.

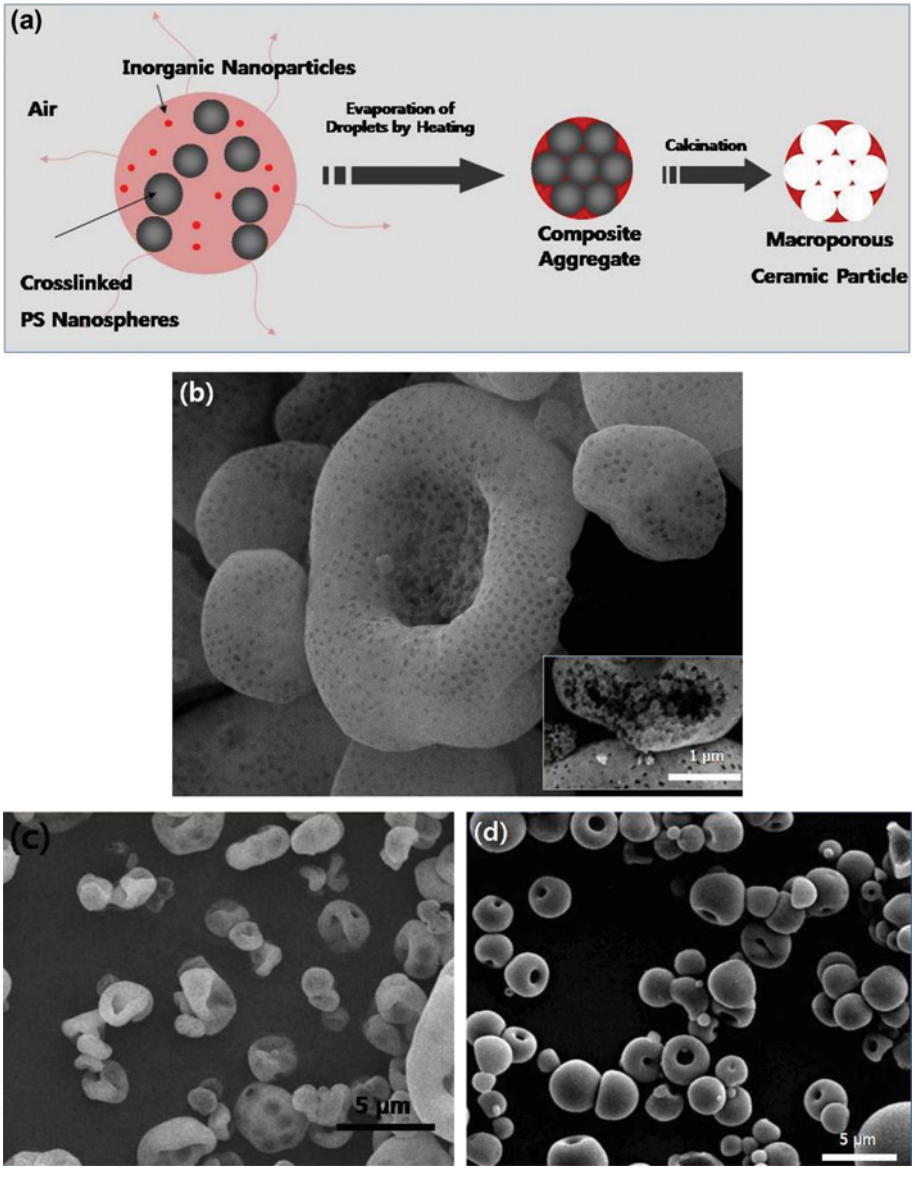

Fig. 9. (a) Schematic figure for the fabrication of porous ceramic particles by aerosol-assisted self-organization and colloidal templating method. SEM image of (b) porous silica and (c) titania particles. Scale bars indicate 1 and 5 μm, respectively. (d) SEM image of titania spheroids fabricated by spray dryer without using PS templates. Scale bar is 5 μm.

Table 1) were mixed for the physical adsorption of the dye; repeated centrifugation was performed to remove unadsorbed molecules from the dispersion as washing step. The resulting dispersion of dye-adsorbed polymeric nanospheres was analyzed by UV-visible spectrometer and the spectrum is contained as dotted line in the graph of Fig. 7(b). Though the peak of absorbance spectrum is not so sharp due to the strong scattering by polystyrene particles, the absorbance peak position of the dye-adsorbed nanospheres coincides with that of aqueous solution of rhodamine B molecules. The third grown particles were also observed using UV-visible spectrometer after the dye adsorption, as displayed in the graph of Fig. 7(c), and the result was similar to the spectrum of Fig. 7(b).

As an application of shape-anisotropic particles displayed in Fig. 4(b), supra-aggregates of the nonspherical particles were fabricated by emulsion-assisted self-assembly strategy described in the schematic of Fig. 8(a). After the nonspherical particles were redispersed in toluene as dispersion medium by centrifugation and sonication, the particle suspension was emulsified into aqueous Pluronic F127 solution by mechanical homogenization. Then, evaporation-driven self-assembly was induced by heating the complex fluid system to prepare supra-aggregates of the nonspherical particles after the removal of the toluene droplets. The morphologies of the resulting supra-aggregates are displayed in the scanning electron microscope image of Fig. 8(b), indicating that the heavy aggregates could be produced from toluene droplets as confining geometries. Since the packing fraction of nonspherical particles is usually larger than that of simple spherical colloids, the supra-aggregates displayed in Fig. 8(b) can be potentially applied for chromatographic applications requiring compactly packed beds for high packing fraction [25].

Besides supra-aggregates of the sea pineapple-shaped particles, porous particles could be produced by employing nonspherical polymeric or seed particles as templates for the formation of macropores. In this study, aerosol-assisted self-assembly scheme was employed to produce porous inorganic particles by spray drying technique, as depicted in the schematic of Fig. 9(a). The inorganic nanoparticles such as silica or titania nano-colloid were used as precursor material for porous backbones, and polymer beads were adopted as sacrificial templates, which were converted into air cavities after calcination. The resulting porous titania particles could be applied as photocatalysts for the removal of organic pollutants from water. Fig. 9(b) contains the scanning electron microscope image of porous silica particles fabricated by spray drying technique. The morphologies of the porous silica particles are highly distorted spheroids, indicating that the evaporation of the droplets produced by two-fluid nozzle of spray dryer was very fast during the drying step. From the SEM image in Fig. 9(b), numerous pores having a cavity size smaller than 160 nm can be observed, implying that colloidal templating method was successful for the fabrication of porous inorganic particles using polystyrene seed particles displayed in the SEM image of Fig. 2(a). The inset SEM image in Fig. 9(b) displays the fractured structure of the porous silica particles, which shows tiny pores exist inside the particles. These porous silica micro-particles can be potentially applied for the adsorption of hydrophilic components such as proteins for various industrial applications since large specific surface area of the powder material can be expected due to the tiny pores in silica backbones. Fig. 9(c) displays the SEM image of macroporous titania particles fabricated using sea pineapple-shaped polymeric beads as templates. From the electron microscope image, the macropores with size of several hundred nanometers can be observed as closed cavities covered with thin titania skin layers. For comparison, titania nano-colloid was solely sprayed without using PS particles, and the resultant titania spheroids after drying are observed by electron microscope, as displayed in Fig. 9(d).

The morphologies of the porous particles were observed by electron microscope and the images are shown in Fig. 9(b) and 9(c). The porous particles have similar morphologies in that there is a hole in the center of the particles. The formation of these highly distorted spheroids can be explained by the rapid evaporation of the aerosol droplets during the spray drying process at high temperature such as 180 °C. Initially, the shape of the droplets is supposed to be spherical, which is the most stable shape minimizing the surface tension. However, rapid evaporation of the droplets

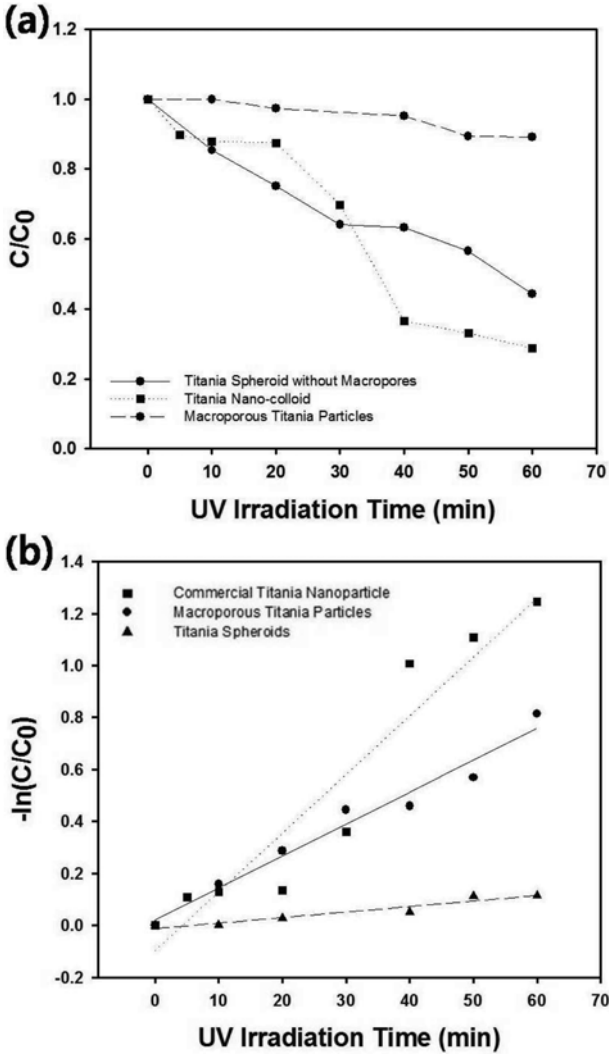

Fig. 10. (a) The change of methylene blue concentration (C/C_0) and (b) $-\ln(C/C_0)$ as a function of UV irradiation time. Macroporous titania particles were used as photocatalytic decomposition reaction.

results in the distortion of the aerosols and the final shape of the porous particles will be donut-like morphologies resembling the SEM images of Fig. 9. Another interpretation can be made using the concept of mass Peclet number, which is defined as the ratio of the migration rate of the colloidal materials inside droplets to the evaporation rate of the droplets.

Fig. 10(a) displays the graph of the change of dye concentration as a function of UV irradiation time. The macroporous titania particles shown in Fig. 9(c) were adopted as photocatalysts for the removal of methylene blue molecules from water. Due to the photocatalytic activity of the porous titania particles, the organic dye molecules could be decomposed under the emission of UV light. The concentration of the model contaminant was reduced with relatively slow rate when titania spheroids without macropores were used as photocatalysts.

To estimate the rate constant of the decomposition reaction, the value of $-\ln(C/C_0)$ was plotted as a function of time, assuming that photocatalytic decomposition reaction is the first order kinetics. From the regression graph of Fig. 10(b), the apparent rate constant was determined as 0.0123 s^{-1}. In this study, the performance of the porous titania particles was compared with commercial titania nanoparticles (Titan PE). When the titania nanoparticles were used, the initial concentration of dye molecules decayed more slowly compared to macroporous particles shown in Fig. 9(c), as displayed in the dotted line of Fig. 10(a). However, the concentration of contaminant was reduced more rapidly when the decomposition time was larger than 40 minutes. This trend can be quantified from the regression line (dotted) of Fig. 10(b), indicating that the rate constant of the titania nanoparticles is 0.0226 s^{-1}, which is larger than that of the macroporous particles. When polystyrene particles were not used as templates, the decomposition of methylene blue was very slow, and the rate constant was determined as 0.0021161 s^{-1}, which was quite small compared to the result of macroporous particles. It is expected that the porous architecture of titania micro-particles displayed in Fig. 9(c) might have contributed the enhanced photocatalytic activities compared to simple titania spheroids, since a large surface area of the porous particles is beneficial to the adsorption of reactant molecules, such as the methylene blue dye. Thus, it can be concluded that the use of polystyrene templates is advantageous for the synthesis of efficient photocatalyst. However, the photocatalytic performance of the commercial titania nanoparticles was better than the results of the other types of micro-particles shown in Fig. 9(c) and 9(d). Since the size of macroporous titania particles is in the micrometer range, the particles are difficult to be absorbed onto human skin layer. However, commercial titania nanoparticles may be transferred more easily inside the human skin, and it is evident that the porous particles can be used as more safe photocatalyst for human health with low toxicity [26].

CONCLUSIONS

Nonspherical polymeric particles resembling sea pineapples were synthesized by successive growth technique using soapless emulsion polymerization method. During the growth step, the spherical shape of the initial seed particles was maintained until the second growth step. The anisotropic nonspherical particles could be obtained by adjusting the amount of monomer during the swelling step in the third growth stage. Composite particles could be also produced by replacing monomer droplets as methylmethacrylate for the synthesis of PS-PMMA particles with raspberry shapes.

As an application of the successively grown particles, the self-organization of the nonspherical particles was studied by observing the supra-aggregates of the particles using an electron microscope. The nonspherical particles could be packed into colloidal aggregates using toluene emulsion droplets as confining geometries. The toluene dispersion containing the sea pineapple-shaped particles was emulsified into aqueous Pluronic F127 solution by mechanical homogenization, followed by the evaporation of the droplets by heating to induce the self-assembly of the particles.

Aerosol-assisted self-assembly strategy was applied for the fabrication of macroporous inorganic particles using spherical seed or sea pineapple-shaped particles as templates by spray drying technique. Evaporation-driven self-assembly scheme was adopted to prepare porous ceramic particles with spherical morphologies after self-assembly and high-temperature calcination. For the porous materials synthesized using latex beads as templates, the conventional pore morphologies have been usually spherical cavities. However, the nonspherical sea pineapple-shaped particles were used as templating materials in this study to prepare porous ceramic particles by aerosol-assisted self-assembly route. The resultant porous particles could be applied as photocatalysts for the removal of organic pollutants from water, and the photocatalytic activity of the porous particles was higher than that of simple titania spheroids without macropores.

ACKNOWLEDGEMENTS

This research was supported by a grant (16CTAP-C114861-01) from Infrastructure and Transportation Technology Promotion Research Program funded by Ministry of Land, Infrastructure and Transport (MOLIT) of Korea Government and Korea Agency for Infrastructure Technology Advancement (KAIA).

REFERENCES

1. H. B. Yamak, Polymer Science, Intech (2013).
2. J. Sakdapipanich, N. Thananusont and N. Pukkate, *J. Appl. Polym. Sci.*, **100**, 413 (2006).
3. Y.-S. Cho, G.-R. Yi, J. H. Moon, D.-C. Kim, B.-J. Lee and S.-M. Yang, *J. Colloid Interface Sci.*, **341**, 209 (2010).
4. L. Xu, H. Li, X. Jiang, J. Wang, L. Li, Y. Song and L. Jiang, *Macromol. Rapid Commun.*, **31**, 1422 (2010).
5. Y. Z. Zhang, J. X. Wang, Y. Zhao, J. Zhai, L. Jiang, Y. L. Song and D. B. Zhu, *J. Mater. Chem.*, **18**, 2650 (2008).
6. Y.-S. Cho, J. H. Moon, G.-R. Yi and S.-M. Yang, *J. Dispersion Sci. Technol.*, **31**, 368 (2010).
7. S. Tabata, Y. Isshiki and M. Watanabez, *J. Electrochem. Soc.*, **155**, K42 (2008).
8. J. Lu, F. Zheng, Y. Cheng, H. Ding, Y. Zhao and Z. Gu, *Nanoscale*, **6**, 10650 (2014).
9. K. Chen and H. Tüysüz, *Angew. Chem. Int. Ed.*, **54**(46), 13806 (2015).
10. J. W. Kim, R. J. Larsen and D. A. Weitz, *Adv. Mater.*, **19**(15), 2005

(2007).
11. D. Kim, D. Y. Lee, K. Lee and S. Choe, *Macromol. Res.*, **17**(4), 250 (2009).
12. M. Pan, L. Yang, B. Guan, M. Lu, G. Zhong and L. Zhu, *Soft Matter*, **7**, 11187 (2011).
13. B. Peng, H. Rao, V. Hanumanth, R. Vutukuri, A. V. Blaaderen and A. Imhof, *J. Mater. Chem.*, **22**(41), 21893 (2012).
14. H. R. Sheu, M. S. El-Aasser and J. W. Vanderhoff, *Polym. Mater. Sci. Eng.*, **57**, 911 (1987).
15. Y.-S. Cho, Y. K. Kim, K. C. Chung and C. J. Choi, *J. Dispersion Sci. Technol.*, **32**, 1408 (2011).
16. Y.-S. Cho, S. H. Kim and J. H. Moon, *Korean J. Chem. Eng.*, **29**, 1102 (2012).
17. Y.-S. Cho, *J. Dispersion Sci. Technol.*, **38**, 159 (2017).
18. D. Nguyen, S. Ravaine, E. Bourgeat-Lamic and E. Duguet, *J. Mater. Chem.*, **20**, 9392 (2010).
19. M. Pan, L. Yang, J. Wang, G. Zhong, M. K. Sen, M. K. Endoh, T. Koga and L. Zhu, *Macromolecules*, **47**, 2632 (2014).
20. C. Tang, C. L. Zhang, J. G. Liu, X. Z. Qu, J. L. Li and Z. Z. Yang, *Macromolecules*, **43**, 5114 (2010).
21. Y.-S. Cho, I.-A. Oh and N. R. Jung, *J. Dispersion Sci. Technol.*, **37**, 676 (2016).
22. P. H. Rogers, E. Michel, C. A. Bauer, S. Vanderet, D. Hansen, B. K. Roberts, A. Antoine Calvez, J. B. Crews, K. O. Lau, A. Wood, D. J. Pine and P. V. Schwartz, *Langmuir*, **21**, 5562 (2005).
23. E. B. Mock, H. D. Bruyn, B. S. Hawkett, R. G. Gilbert and C. F. Zukoski, *Langmuir*, **22**(9), 4037 (2006).
24. E. D. Emmons, R. G. Kraus, S. S. Duvvuri, J. S. Thompson and A. M. Covigton, *J. Polym. Sci. B, Polym. Phys.*, **45**, 358 (2007).
25. A. Donev, I. Cisse, D. Sachs, E. A. Variano, F. H. Stillinger, R. Connelly, S. Torquato and P. M. Chaikin, *Science*, **303**, 990 (2004).
26. M. Crosera, M. Bovenzi, G. Maina, G. Adami, C. Zanette, C. Florio and L. F. Filon, *Int. Arch. Environ.*, **82**(9), 1043 (2009).